Laser Beam Welding of Aluminum Alloy 5456

More than 90% of precipitates are vaporized during laser irradiation to enhance the toughness of the laser weld

BY D. W. MOON AND E. A. METZBOWER

ABSTRACT. Using a high power laser, ½ in. (12.7 mm) thick plates of aluminum alloy Al 5456 were butt welded.

The redistribution of solutes and precipitates in the fusion zone was investigated and correlated with the enhanced toughness of the laser beam weldment.

Metallographic examinations indicated both substantial purification and refined grain structures in the fusion zone.

Electron microprobe studies revealed a gradual decrease in Mg concentration from the fusion boundary towards the center of the weld and an increase in the concentrations of Cr, Mn and Al in the weld center.

Dynamic tear (DT) tests disclosed that the DT value of the laser beam weldment is superior to that of the base metal plate. The fractographic observations revealed that the fracture process was microvoid coalescence. The enhanced fracture toughness is due primarily to the evaporation of precipitates during laser beam welding.

Introduction

The development of high density heat sources is a continuing effort in the area of fusion welding. In the past, the electric arc has been used as a relatively high density heat source. More recently, the electron beam provided a more concentrated source of heat, but it usually requires a vacuum. The laser provides a similar high intensity heat source without the need of a vacuum system. The most useful high power laser for welding is the CO_2 gas laser. Radiation is in the far infrared region of the spectrum at a wave length of 10.6 μm.

Two important consequences of welding with a high intensity heat source are rapid solidification and keyhole type of penetration. The temperature gradient between the heat source and the workpiece increases as the energy density in the beam increases. The steep temperature gradient causes rapid cooling, producing fine structures and improved weldment properties.

At the surface of the metal the focused laser beam causes the metal to vaporize, producing a column of vapor extending deep into the base metal. During this time particles are evaporated and aspirated. It is well known that as the volume fraction of inclusion increases, toughness decreases (Refs. 1-3). The laser beam weld metal thus will have enhanced fracture toughness. This purification phenomenon (Ref. 4) is one of the advantageous aspects of laser welding.

The aim of the investigation described here is to study the vaporization of precipitates during laser irradiation and to correlate this phenomenon to the mechanical properties and the fracture toughness of the laser beam weldments.

The aluminum alloy studied in this investigation was 5456-H116. This aluminum-magnesium alloy is characterized by good mechanical properties, high corrosion resistance and good weldability. It is specified for marine applications. The H116 temper was developed specifically to eliminate exfoliation in marine environments (Ref. 5).

The mechanical properties and the toughness of the laser beam weldments will be correlated with the metallographic and fractographic examinations. The redistribution of alloying elements and precipitates during laser beam welding will also be studied to evidence the relationship between the toughness and fusion zone purification of the laser weldment.

Experimental Procedures

Laser Welding

A continuous wave carbon dioxide laser in the unstable resonator mode was used for these experiments. The horizontal output beam from the laser was reflected upward by a plane mirror into a downward facing focusing mirror to provide downhand welding conditions. The power density at the 8 kW power level was approximately 10^6 watt/cm^2 at the workpiece surface.

The welds were made by moving the workpiece on the table under a stationary laser beam. The plate surfaces to be welded were machined for a square butt joint configuration and roto-blasted. Then the joint areas were wiped with acetone. Helium gas was used to shield the workpiece. The gas shielding arrangement consisted of four channels:

1. A leading shielding gas applied through porous metal in front of the molten pool.
2. Trailer shielding gas behind the weld pool to protect the hot, newly solidified weld metal as it emerged from the laser beam.
3. Bottom shielding gas bled into the groove of a fixture to shield the underbead.
4. Plasma shielding gas that flowed normal both to the beam path and the direction of the weld progress.

The purpose of the plasma shielding gas was to blow plasma, fumes and other contaminants away from the molten pool, thereby allowing the laser beam to interact directly with the workpiece without being absorbed by the plasma. This results in increased penetration capability of the laser beam.

Figure 1 shows a laser welding station

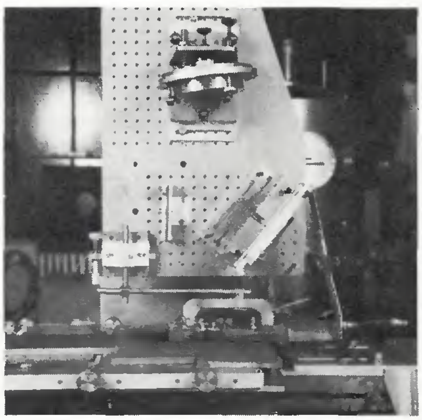

Fig. 1—Laser beam welding station

Paper presented at the 63rd Annual AWS Convention in Kansas City, Missouri, during April 25-30, 1982.

D. W. MOON and E. A. METZBOWER are with the Naval Research Laboratory, Washington, D.C.

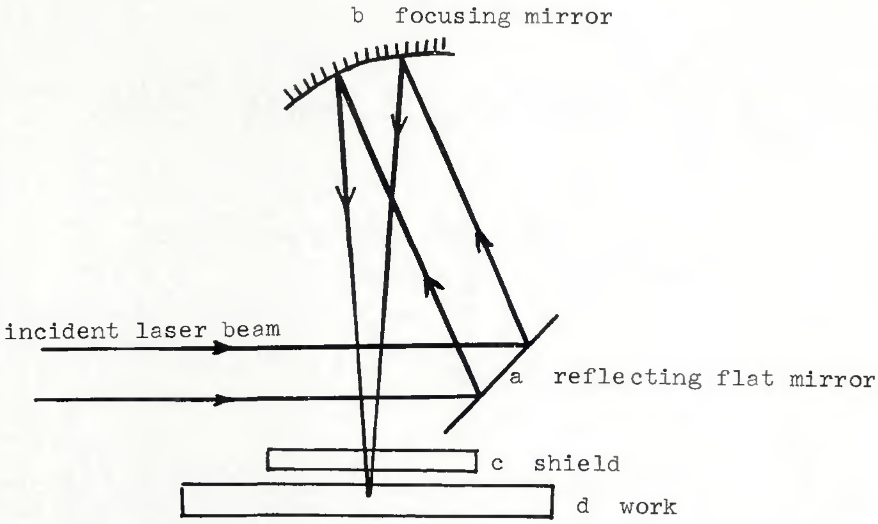

Fig. 2 — Schematic of laser welding station

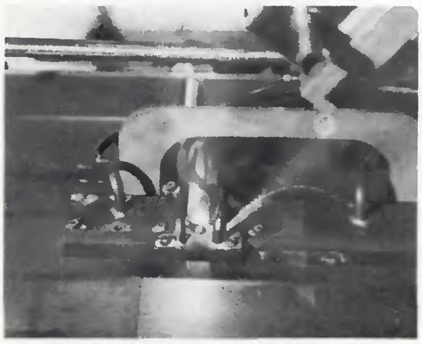

Fig. 3 — Close-up of the shield and workpieces during laser beam welding

comprised of (a) a reflecting flat mirror, (b) a focusing mirror, (c) a shield and (d) workpieces positioned on the table. A corresponding schematic is shown in Fig. 2. Figure 3 shows a close-up of the shield and workpieces during laser beam welding.

Precise alignment of the joint to be welded was made using a helium-neon laser which is made coincidental with the CO_2 laser beam. The He-Ne laser beam has a visible red color and a safe power level of 5 mW. During alignment, clamping forces were exerted on the sides of the workpieces by a series of screw threads to ensure the parts being forced solidly against one another. Prior to welding, tack welds were made on both ends of the joint to be welded to prevent relative movement between the two plates due to expansion and contraction of the plates during welding.

Two 0.5 in. (12.7 mm) thick plates of 4 × 8 in. (102 × 203 mm) aluminum alloy 5456 were square butt welded without filler metal. Nominal composition of the base plate is presented in Table 1, and welding parameters are given in Table 2.

Tensile Test

Transverse weld tension specimens were prepared with circular cross sections. The weld bead location was centered along the longitudinal axis of the specimen. Elongation was measured using a 1 in. gage length extensometer which straddled the weld at the specimen center line. Load-elongation curves were obtained using an X-Y recorder. From these data the ultimate tensile strength, yield strength at 0.2% offset and % elongation were calculated.

Dynamic Tear (DT) Tests and Fractography

A double pendulum machine of 2712 N-m (2,000 ft-lb) capacity was used to measure room temperature fracture toughness of the weldments. A narrow, 1/16 in. (1.6 mm) deep notch was machined and then sharpened by a pressed knife-edge, producing a deep, sharp crack. The thickness of the DT specimen was 12 mm (0.5 in.) instead of the 16 mm (5/8 in.) thickness normally used as a standard DT specimen. Fracture surfaces of the DT test specimens were then examined in a field emission scanning electron microscope.

Metallography

Transverse cross sections were cut from the weldments for metallographic examination. Specimens were polished with diamond powder less than 1 μm diameter and etched electrolytically with the A-2 solution of the Knuth system for the microstructural study. As-polished, unetched specimens were used for the study of the redistribution of the solutes and precipitates.

In order to compare precipitates in the fusion zone and the base metal, a montage was made containing the entire area of the fusion zone and its equivalent area of the base metal. The size of the counted precipitates was approximately 15 μm or greater.

Table 1—Nominal Composition of Aluminum Alloy 5456 Base Metal, Wt-%

Magnesium	5.25	Chromium	0.10
Manganese	0.80	Aluminum	Balance

Table 2—Laser Beam Welding Parameters

Power, kW	8.0
Speed, mm/s	27.5
(ipm)	(65)
Heat input, kJ/mm	0.29
(kJ/in.)	(7.4)

Electron Beam Microprobe Analysis

A transverse cross section of the weldment was prepared for microprobe analysis. The section was polished with 1 to 5 μm diamond powder and then 0 to 1 μm diamond powder. The upper portion of the cross section was photographed at low magnification (×30) as a guide and the region of interest was identified by suitably located microhardness indentations.

The as-polished specimen was scanned from one side of the base metal, across the fusion zone, to the other side of the base metal. The intensity of the characteristic radiation from hemispherical volume of 1 μm diameter excited by a 0.1 μm diameter stationary beam was measured. With the aid of suitable standards, the radiation counts per unit time (cts/sec) were converted to weight-% values for Al, Mg, Mn and Cr. X-ray images of the microprobe specimen were also made to identify the representative precipitates common to the base metal.

Table 3—Mechanical Properties(a) of Al 5456-H116

Alloy	σ_{ys}, MPa (ksi)	σ_{ult}, MPa (ksi)	El, %	DT energy, N.m (ft-lb)
Base metal	255 (37)	351 (51)	16.0	98.9 (73)
Laser weld	193 (28)	289 (42)	9.2	116.5 (86)
GMA weld	158 (23)	317 (46)	14.0	162.6 (120)

(a) ys — yield strength; ult — ultimate tensile strength; El — elongation.

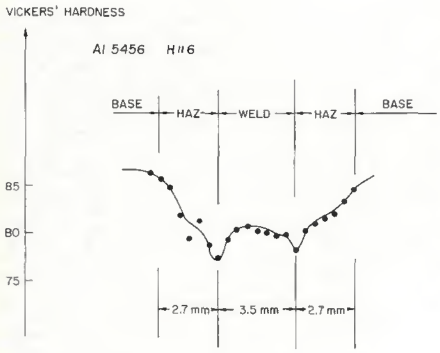

Fig. 4—Hardness traverse of Al 5456 laser weld

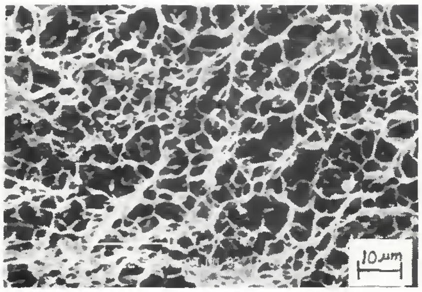

Fig. 5—Fracture surface of DT specimen

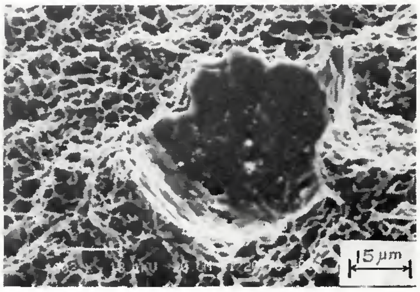

Fig. 6—Typical pore of the fracture surface of a DT specimen of a laser weld

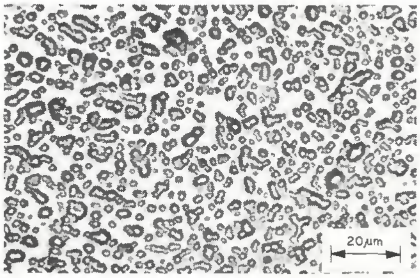

Fig. 7—Fine grained Al solid solution in fusion zone of Al 5456 laser weldment. Etched in A-2 solution of the Knuth system. Hardness—80 HV

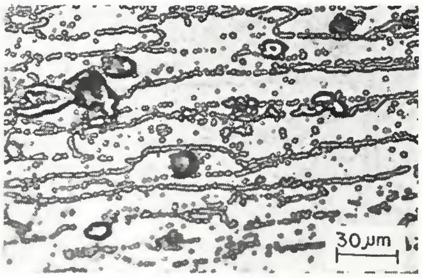

Fig. 8—Strain-hardened, elongated α aluminum and β $Al(Mg_2Al_3)$ in base metal plate of Al 5456-H116. Etched in A-2 solution of the Knuth system. Hardness—87HV

Results

Mechanical Properties

The mechanical properties of the laser beam weldments are compared with those of base plates and of GMA weldments in Table 3. In general the tensile mechanical properties of the laser beam weld are poorer than the base metal properties. Fracture toughness values are also compared in the table. All of the laser beam weld tensile test specimens failed not in the base metal, but in the fusion area. The ductility of the laser beam weldments is also reduced from the value of the base metal. This is primarily due to the porosity which is observed on the fracture surfaces. On the other hand dynamic tear test energies of the laser welds (86 ft-lb) have improved from the value of the base plate (73 ft-lb). This is attributed to intense high energy laser beam. This matter is further explored in the discussion.

The reduction in strength of the laser weldment is well reflected in the hardness behavior. Strength in aluminum alloys increases with hardness (Ref. 6) as in ferrous alloys. Figure 4 shows a hardness traverse from one side of the base metal, across the fusion zone, to the other side of the base metal.

The Vicker's values vary from 87.0 in the base metal to 77.5 in the HAZ adjacent to the weld-HAZ interface. The average hardness value of the fusion zone is approximately 80.0 HV. The material is gradually softened from the strain hardened state to the fusion boundary where the strain hardening is severely destroyed by the laser heat input. The lower hardness values of the fusion zone are simply the result of unstrained cast structure and also of Mg loss. Since Al 5456 alloy is non-heat treatable, it is not surprising to find this hardness behavior. The reduced hardnesses in the HAZ and the fusion area, and the considerable porosity in the fusion zone, explain the degraded mechanical properties of the laser beam welds.

Fractography

Fractographic observations of the DT

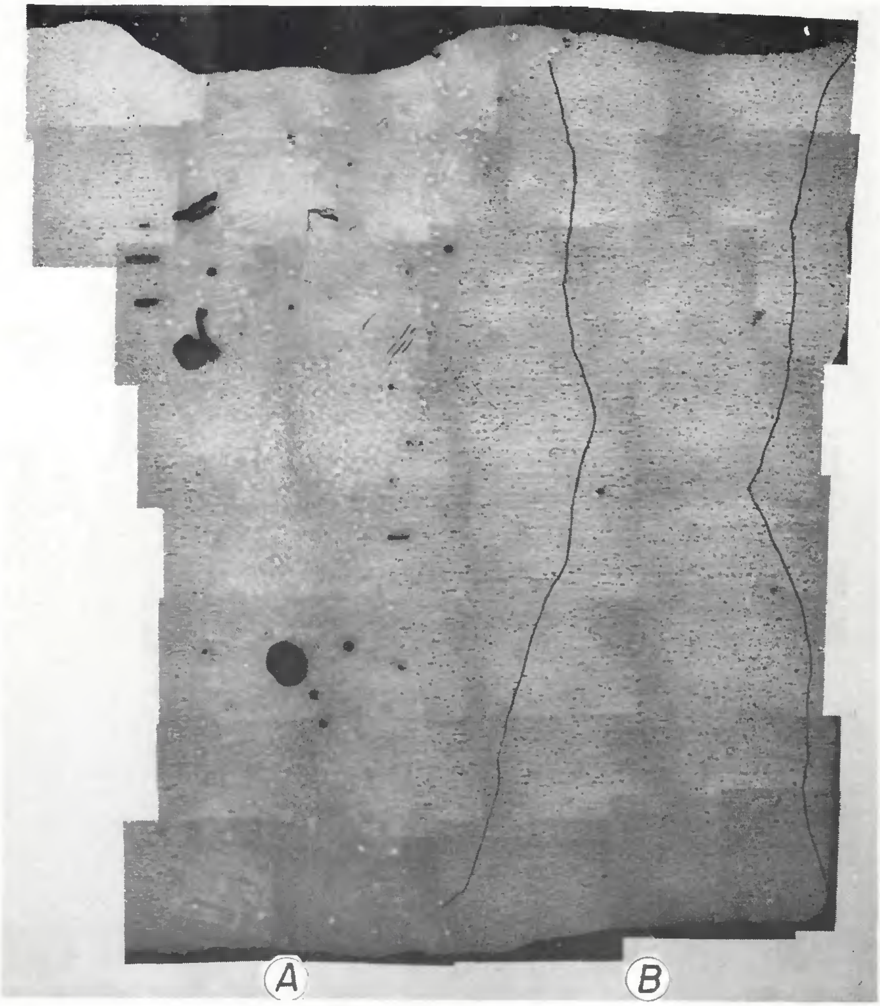

Fig. 9—Montage exhibiting the redistribution of precipitates during laser welding: A—fusion zone; B—equivalent area in base metal

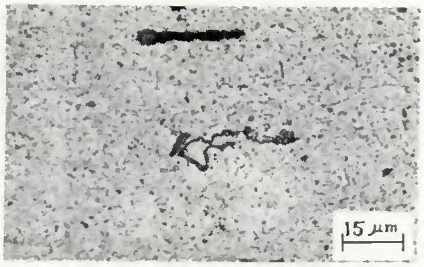

Fig. 10 — Photomicrograph of typical precipitates in base metal

specimens correlate well with the DT values. Figure 5 shows a fractograph of a DT specimen, indicating that the fracture separation process was microvoid coalescence.

On the other hand the fractographic study also revealed an appreciable amount of porosity as shown in Fig. 6.

Metallography

Representative microstructures of the fusion zone and the base metal are shown in Figs. 7 and 8. The microstructure of fusion zone is considerably finer than that for the base metal. This is attributed to the fact that laser beam is a very high density power source. The temperature of the melt thus gets very high, and the temperature gradient between the melt and the base metal becomes extremely steep. The steep temperature gradient causes a high cooling rate, producing fine microstructure. In addition to the fine structure, the fusion zone became remarkably cleaner compared to the base metal in terms of inclusions.

Precipitates of approximately 15 µm or above were counted visually both in the fusion zone marked A in Fig. 9 and in an immediately adjacent equivalent area in the base metal marked B in Fig. 9. Precipitate counts were 3 in the fusion area and 58 in the base metal. Only 5% of the insoluble particles are retained in the fusion area after laser beam welding. Although the visual counting method was not precise, it was sufficient to demonstrate the purification mechanism.

Figure 9 consists of a montage depicting the redistribution of precipitates. The elements of those particles were identified by microprobe analysis.

X-Ray Images of Microprobe Specimen

An optical photomicrograph of typical precipitates in the base metal is shown in Fig. 10, and the corresponding x-ray patterns of these precipitates are given in Fig. 11.

There are two large precipitates common to the base metal in Fig. 10; the black particle of about 20 µm is Mg_2Si with some iron. The gray one of about 30 µm is a precipitate of $(Fe,Mn)Al_6$ complex as shown by the x-ray images of each element. The identification of precipitates above agrees well with the works reported by others (Ref. 7 and 8).

Redistribution of Solutes

Metallographic study showed a drastic reduction in precipitates in the fusion zone. This is due to the intense high energy laser beam. One can thus reasonably expect evaporation of precipitates and solutes with very low boiling temperatures during laser welding. In fact, the electron microprobe analysis revealed this phenomenon.

The solute redistributions of the major alloying element, Mg, along with that of Al are shown in Fig. 12. The concentration of Mg decreased gradually from the fusion boundary to the weld center by 0.9 wt-% and then increased back to the nominal composition of the base metal approaching the fusion boundary. On the other hand, the other alloying elements — Mn, Cr, and Al — increased in concentration from the base metal approaching the center of the weld: Al by 0.92%, Mn by 0.10%, and Cr by 0.03%, as shown in Table 4. Experimentally obtained compositions of the base

Table 4—Compositional Changes

Elements	Base metal, c/s	Weld center, c/s	Intensity change, %	Change, wt-%
Al	2054	2076	+1	+0.92
Mg	100	88	−12	−0.90
Mn	38	45	+17	+0.10
Cr	11	14	+25	+0.03

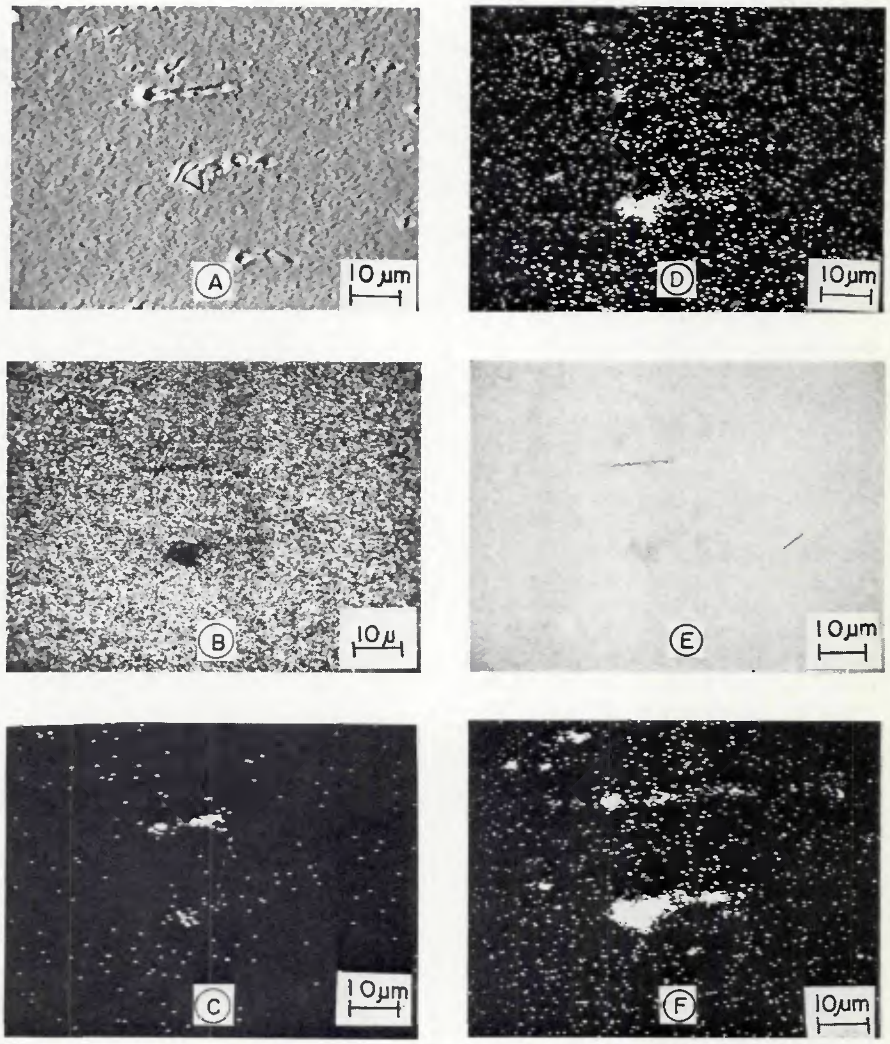

Fig. 11 — X-ray patterns of precipitates: A — secondary electron display of precipitates; B — Mg x-rays; C — Si x-rays; D — Mn x-rays; E — Al x-rays; F — Fe x-rays

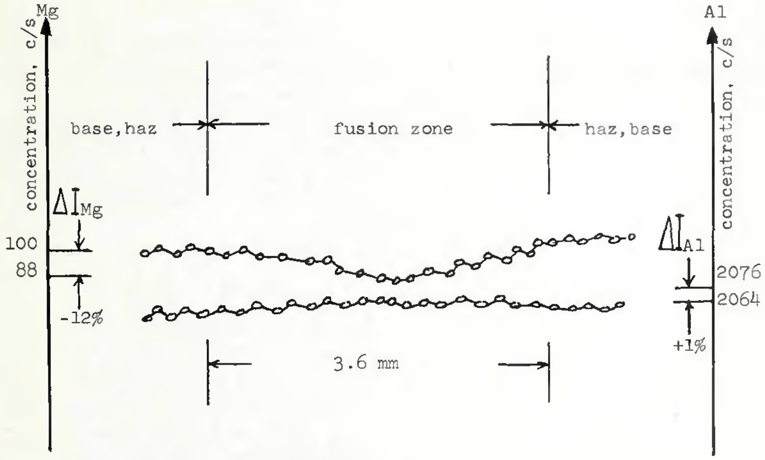

Fig. 12 — Concentration profile of Mg and Al

Table 5—Experimentally Obtained Compositions, Wt-%

	Base metal	Weld center
Al	94.15	95.07
Mg	5.30	4.40
Mn	0.45	0.55
Cr	0.10	0.13

Table 6—Vaporization and Melting Temperatures[(a)]

Elements	T_b (evaporation temperature), °C	T_m (melting temperature), °C
Al	2467	660.4
Mg	1090	648.8
Mn	1962	1244.0
Cr	2672	1857.0

(a) $°F = \frac{9}{5}°C + 32$.

metal are compared to those of the laser weld center in Table 5.

Figure 13 compares the concentration change of Mn with that of Mg. In a similar fashion the compositional variations of Cr and Mg are shown in Fig. 14. The change in x-ray count intensity corresponding to the change in concentration, ΔI, was converted with weight-%, as shown in Table 4.

The reduction in concentration of Mg in the fusion zone is attributed to its low evaporation temperature. Notice, in Table 6, that the boiling points of Mg and Al are 1090°C and 2467°C (1994°F and 4473°F), respectively; thus, the difference is almost 1300°C (2372°F). Notice also, in Table 6, that the melting points of Mn and Cr are 1244 and 1857°C (2271 and 3375°F). Therefore, at temperatures of about 1100°C (2012°F), Mg already has reached the boiling point, while the other alloying elements, Mn and Cr, have not yet even melted. The increase in concentration of Al is due to the depletion of Mg. The compositional increase in Mn and Cr is attributed to solute segregation during welding solidification, in addition to the evaporation of Mg.

In considering the vaporization of precipitates, the vaporization and melting temperatures of the precipitates should be considered rather than the values of individual elements of which a precipitate consists. The reason is that the vaporization temperature of a precipitate may be different from the superposition of vaporization temperatures of each of the elements of the precipitate. Unfortunately, the vaporization and melting temperatures of the precipitates are not available in the literature.

Discussion

Degradation of Mechanical Properties

Mechanical properties of Al 5456-H116 weldments are degraded during laser welding. There are three major causes for this: depletion of magnesium; loss of strain-hardened structure; and porosity formation. These are discussed in turn below.

Depletion of Magnesium. Magnesium is the major alloying element for 5000 series of aluminum alloys; and the strengthening of these alloys is primarily by solid solution of magnesium in the aluminum matrix. Evaporation of magnesium was observed in the microprobe study.

The relationship between Mg content and the tensile strength of Al-Mg alloys was established by the Aluminum Association as shown in Fig. 15 (Ref. 9). Figure 15 shows that the tensile strength of Al-Mg alloy increases with Mg content. Similar studies on the effect of Mg content on the strength and hardness in Al alloys are also reported in the literature (Ref. 10 and 11). The Mg atom is larger than the Al atom and sets up a compressive strain field in an Al-Mg solid solution. Thus the presence of Mg atoms impedes dislocation motion, increasing yield strength.

In Fig. 15 the tensile strength dropped by approximately 7 ksi (48 MPa) as Mg content decreased from 5% to 4%. In our experiment we also observed approximately 9 ksi (62 MPa) reduction in strength (Table 3) corresponding to 1% magnesium reduction from approximately 5% to 4% (Table 5). Figure 15 shows only a trend and care should be made of its quantitative application to our case; although the two systems are very similar.

It is obvious that evaporation of alloying elements causes degradation of weld

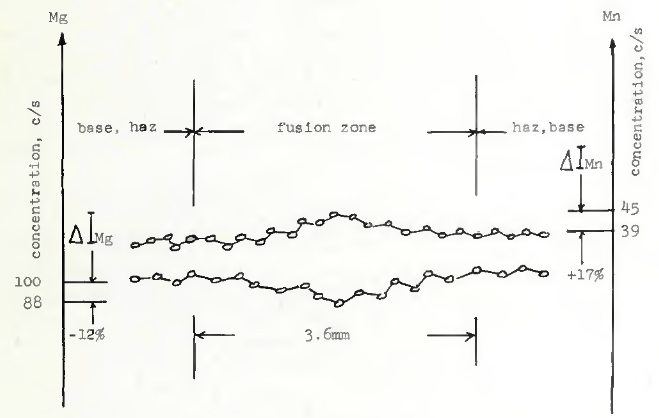

Fig. 13 — Concentration profile of Mg and Mn

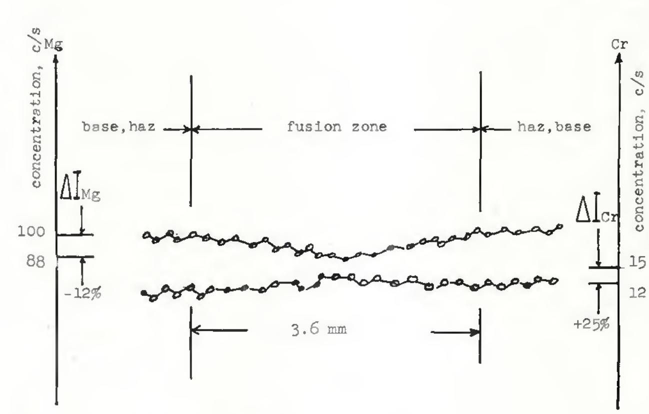

Fig. 14 — Concentration profile of Mg and Cr

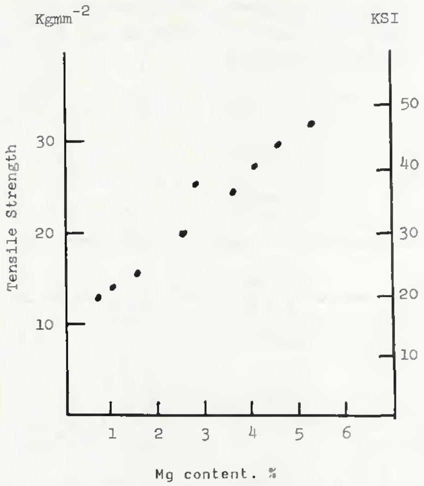

Fig. 15 — Tensile strength of Al-Mg alloys vs. Mg content (Ref. 6)

properties. One way of diminishing vaporization of alloying elements could be by reducing the power level at the expense of welding speed. In the case of filler metal application, it is recommended that the Mg content in the filler metal be increased in order to compensate for the vaporized Mg content in the fusion zone.

Both Cr and Mn are added to improve resistance to stress corrosion cracking and also increase tensile strength (Ref. 12). Although increases in the Mn and Cr contents are found in the weld (Figs. 13 and 14), it is negligible compared to the depletion of Mg. Therefore, increased tensile strength due to increased Mn and Cr would also be insignificant.

Loss of Strain-Hardened Structure. The second cause responsible for the poor tensile properties of the weld is believed to be the destruction of strain-hardened structure. In addition to solid solution strengthening mechanism, Al 5456-H116 is further strengthened by strain aging as the H116 temper indicates. During melting, the strain-hardened structure is completely destroyed and becomes a cast structure with lower hardness and lower strength.

Porosity Formation. The third factor is porosity formation during laser irradiation. One of the major problems with aluminum welding, even in conventional processing, is pore formation during solidification. Hydrogen is the only gas known to be measurably soluble in either solid or molten aluminum. The solubility of hydrogen dissolved in the atomic state is approximately 20 times greater in liquid than in solid aluminum. Because of this solubility difference, the atomic hydrogen tends to come out of solution during solidification, forming molecular hydrogen either by slow diffusion or by rapid formation of bubbles. Since laser welding is a rapid cooling process, the probability is higher that the gases will be trapped in the solidifying weld metal (Ref. 13).

It is relatively well established that porosity diminishes the tensile strength of a metal. Lawrence, et al. investigated the effects of porosity on Al-5000 series and Al-6000 series alloy welds and concluded that weld porosity was detrimental to the tensile strength as well as the ductility of the weld (Ref. 14). Similar work on Al-5086 alloy welds was also reported by Ashton, et al. (Ref. 15).

Toughness

The tensile properties of laser beam welds are poor — that is, the laser beam welds were inferior not only in tensile strength, but also in ductility, to the base metal as shown in Table 3. Also observed was appreciable porosity on the fracture surface as shown in Fig. 6. Nevertheless, the measured DT energy of the laser weld of Al 5456-H116 alloy is superior to that of the base metal. Fractographic observations revealed, as shown in Fig. 5, that the fracture separation process was microvoid coalescence, demonstrating good toughness of the laser weld. What then is attributed to enhanced toughness? There are positive and negative factors to this as discussed below under separate headings.

Negative Factor. In their extensive investigation on the effects of porosity on the fracture toughness of Al-Mg alloy weldments, Lawrence, et al. (Ref. 14) concluded that there is a definite relationship between the fracture energy and the total porosity, the fracture energy decreasing with an increase in total porosity. Large amounts of porosity found in the DT specimens led us to conclude that porosity is harmful to the fracture toughness of Al 5456 laser weld. The effects of porosity on fracture toughness deserve further indepth study.

Positive Factors. High energy laser irradiation causes the precipitates in the fusion area to vaporize approximately 95% during laser welding as shown in Fig. 9. This purification phenomenon is the primary contribution to good toughness of the laser weldment of Al 5456-H116 alloy. In addition to this major beneficial effect, a considerably refined weld structure due to rapid solidication and also the reduced yield strength of the laser weld (Ref. 16) should also contribute to some extent to the enhanced DT energy.

As a result of this experiment, the feasibility of welding aluminum alloy with laser has been demonstrated. Further refinement of technique to optimize joint properties remains to be made.

Conclusions

1. The Mg content is lower in the center of the fusion zone than at the fusion boundary.
2. More than 90% of the precipitates are vaporized during laser beam welding.
3. Both the tensile strength and ductility of the laser beam weldments are lower than the base metal properties.
4. The toughness values (DT energy) of the laser beam weldments are superior to the base plate values due to the fusion zone purification mechanism and refined structures.

Acknowledgments

The authors are grateful to E.A. Pierpoint for the mechanical testing of the weldments. Technical assistance and valuable comments on the probe work by E.J. Brooks and F.W. Fraser is also deeply appreciated.

References

1. Edelson, B. I., and Baldwin, W. M. 1962. The effect of second phases on the mechanical properties of alloys. *Trans. ASM* 55:230.
2. Gladman, T., Holmes, B., and McIvor, I. D. 1971. *Effects of second phase particles on strength, toughness and ductility.* Iron and Steel Institute rept. no. 145.
3. Gray, J. M., and Wilson, W. G. 1973. Evaluation of an X-80 arctic pipeline steel containing 0.10% columbium. Paper presented at Petroleum Mechanical Engineering Conference, ASME.
4. Breinan, E. M., and Banas, C. M. 1975. Fusion zone purification during welding with high power CO_2 lasers. *Proceedings of the second international symposium of the Japan Welding Society,* Osaka, Japan, Aug. 24-28.
5. Bogar, F. O. and Crooker T. W., 1977 (October). *Effects of natural seawater and electrochemical potential on fatigue crack growth in 5086 and 5456 Al alloys.* NRL report 8153, p. 1.
6. Mondolfo, L. F. 1976. *Aluminum alloys,* pp. 315 and 369. Butterworth & Co. Ltd.
7. American Society for Metals. Atlas of microstructures of industrial alloys. *Metals handbook* vol. 7, 8th ed., p. 244. Metals Park, Ohio.
8. Bogar, F. D., and Crooker, T. W. *Effects on natural seawater and electrochemical potential on fatigue-crack growth in 5086 and 5456 aluminum alloys.* NRL report 8153, p. 9.
9. Aluminum Association. *Aluminum standards and data.* New York. Also: Mizuno, M., and Nagaoka, H. 1979. Application of Al-Mg alloys to large welded structures in Japan. *International Metals Review* 2:68.
10. Mondolfo, L. F. 1979. *Aluminum alloy,* p. 315.
11. Van Horn, Kent R., ed. 1967. *Aluminum,* vol. I, p. 196.
12. Mizuno, M., and Nagaoka, H. 1979. Application of Al-Mg alloys to large welded structures in Japan. *International Metals Review* 2:72.
13. Van Horn, Kent R., ed. 1967. *Aluminum,* vol. III, p. 29. Metals Park, Ohio: American Society for Metals.
14. Lawrence, F. V., Jr., and Munse, W. H. 1973. *Effects of porosity on the tensile properties of 5083 and 6061 aluminum alloy weldments.* WRC bulletin 181, p. 7. New York: Welding Research Council.
15. Ashton, R. F.; Wesley, R. P.; and Dixon, C. R. 1975. The effect of porosity on 5086-H116 aluminum alloy welds. *Welding Journal* 54(3):95-s to 98-s.

American Welding Society P.O. Box 351040, Miami, FL 33135 Telex: AMWELD SOC No: 51-9245
(305)642-7090

AN INVITATION TO AUTHORS

to present Brazing Papers at the
15th AWS-WRC International Brazing and Soldering Conference
Dallas, Texas, April 10–12, 1984

The American Welding Society's C3 Committee on Brazing and Soldering invites you to present your outstanding and unpublished work in the field of brazing development, research or application at the 15th International AWS-WRC Brazing and Soldering Conference. This event will be held in conjunction with the Society's 65th Annual Convention at the Dallas Convention Center, Dallas, Texas.

Please submit your abstract(s) by August 15, 1983, to be screened by the Papers Selection Committee for the 1984 conference. Authors will be notified sometime in November, 1983, regarding acceptance of their papers.

Each abstract should be sufficiently descriptive to give a clear idea of the content of the proposed paper. In any case, it must contain not less than 500—*but preferably not more than 1000*—words. Manuscripts of approximately 5,000 words must be submitted before final approval is given. Repeated references to a company and/or the use of advertisement, trade names, trade marks (or expressions considered as such by the industry) are not permitted. Suitable generic terms must be used, in accordance with those standardized by the American Welding Society, where applicable.

Papers may be considered for publication in the *Welding Journal* regardless of acceptance for presentation at the conference. Topics of particular interest in brazing are:

Applied technologies of (1) aerospace structures, (2) machine tools, (3) nuclear assemblies, (4) automotive assemblies, (5) electronic equipment, (6) food processing equipment and (7) pressure vessels. Of special interest is the application of brazing to titanium, aluminum and other base metals including brazement strength data.

New research and development on (1) brazing filler metals, (2) brazing filler metal-base metal interaction, (3) nuclear properties of brazements (4) electronic properties of brazements, (5) corrosion of brazements and (6) strength of brazed joints.

In addition, papers dealing with educational and informative aspects of brazing production, engineering, research and metallurgy are welcomed if the subject falls within the scope of the session.

Please fill out the Author's Application Form (reverse side), attach abstract thereto and return to AWS. To assure your paper's consideration for the 1984 conference, your abstract must be postmarked *no later than August 15, 1983.*

Paul W. Ramsey

Paul W. Ramsey
Executive Director

IMPORTANT: ABSTRACTS MUST BE AT LEAST 500 WORDS AND BE POSTMARKED NO LATER THAN AUGUST 15, 1983, TO ASSURE CONSIDERATION.

AUTHOR APPLICATION FORM FOR BRAZING PAPERS

DEADLINE AUGUST 15, 1983

Complete in Full and Return to American Welding Society, Inc., P.O. Box 351040, Miami, Florida 33135

Date Mailed ....

Author's Name ....

Company or Operation ....

Title or Position ....

Mailing Address ....

City .... State .... Zip ....

Telephone (including Area Code) ....

If there are to be joint Authorships, give name(s) of other author(s)

Name ....

Address ....

Name ....

Address ....

Proposed title (10 words or less):

____

____

ABSTRACT:

- Type, double spaced, an abstract of *not less than 500—but preferably not more than 1000*—words on separate sheets and attach to this form.
- Be sure to give sufficient information to enable the Papers Selection Committee to obtain a clear idea of content of the proposed paper; confine background to about 100 words. Also be sure to *emphasize Results and Conclusions* since this material, together with information on what is NEW, will have a very important bearing on the final decision of the Papers Selection Commitee.
- If complete manuscript is available, in addition to abstract, please attach two copies to this form.
- Application Form and Abstract must be postmarked not later than August 15, 1983, to assure consideration.

MANUSCRIPT DEADLINES:

- All manuscripts *must* be in the hands of the Papers Selection Committee no later than March 15, 1984. If received by that date, every effort will be made to publish them in a special Brazing and Soldering issue.
- It is expected that the Committee's selections will be announced sometime in November, 1983.
- If your paper is made a part of the program, which of the following manuscript deadlines will you be able to meet?
  December 15, 1983 ☐ January 14, 1984 ☐ February 15, 1984 ☐

PRESENTATION AND PUBLICATION OF PAPERS:

- Has material in this paper been previously presented in meeting or published?
  Yes ☐ No ☐ When? ________ Where? ________
- Following presentation at the *Conference,* would you accept invitations to present this paper before AWS Sections? Yes ☐ No ☐
- Papers accepted for presentation become the property of the Society with original publication rights assigned to the *Welding Journal.*

RETURN TO AWS HEADQUARTERS. MUST BE POSTMARKED ***NOT LATER THAN AUGUST 15, 1983,*** *TO ENSURE CONSIDERATION.*

____

Author's Signature